ISSN 0020-4412, Instruments and Experimental Techniques, 2026, Vol. 69, No. 1, pp. 160–165. © Pleiades Publishing, Ltd., 2026.

PHYSICAL INSTRUMENTS FOR ECOLOGY, MEDICINE, BIOLOGY

Measuring Proton Beam Parameters Using Boron-Enriched Plastic Scintillators

T. A. Bykov[a,*], G. D. Verkhovod[a,], V. V. Porosev[a,b,***], S. Yu. Taskaev[a,b,****], and A. E. Shemyakov[c,*****]**

[a] *Budker Institute of Nuclear Physics, Siberian Branch, Russian Academy of Sciences, Novosibirsk, 630090 Russia*

[b] *Novosibirsk State University, Novosibirsk, 630090 Russia*

[c] *Physicotechnical Center, Lebedev Physical Institute, Russian Academy of Sciences, Protvino, Moscow oblast, 142281 Russia*

**e-mail: timaisabrony@gmail.com*

***e-mail: g.verkhovod@alumni.nsu.ru*

****e-mail: porosev@inp.nsk.su*

*****e-mail: taskaev@inp.nsk.su*

******e-mail: alshemyakov@yandex.ru*

Received August 25, 2025; revised September 8, 2025; accepted September 18, 2025

Abstract—The presented work reports the results of measuring the spatial distribution of proton and secondary particle fluxes at the Prometheus proton therapy facility of the Physico-technical Center, Lebedev Physical Institute, and gives a comparison with simulation results obtained using the Geant4 software package. Measurements conducted with a water phantom, as well as with a compact neutron detector based on a boron-enriched scintillator developed at the Budker Institute of Nuclear Physics, demonstrated good agreement between the observed neutron fluxes and the simulations. The simulation data suggest that the mechanism of enhanced biological effectiveness observed in several studies during proton irradiation with the use of boron-containing compounds is questionable, given the significantly lower contribution to the radiation dose from alpha particles compared to the dominant component caused by protons and other reaction products.

Keywords: neutron detectors, devices for biology and medicine

DOI: 10.1134/S0020441226700089

1. INTRODUCTION

Boron neutron capture therapy (BNCT) is a method of selectively destroying tumor cells that have accumulated the boron-10 compound by irradiating them with a flux of epithermal neutrons. The intense neutron fields required for patient irradiation at BNCT facilities do not allow the measuring detectors and their electronics to be placed directly near the generating source. The most viable solution has proven to be one using a neutron-sensitive scintillator and reading the generated light via optical fiber [1, 2]. Similarly, with a small-sized neutron detector (the size of the sensitive element is approximately 1 mm^3) based on a fast polystyrene scintillator developed at Budker Institute of Nuclear Physics, simultaneous measurement and continuous monitoring of the absorbed dose rate of the nuclear reaction $^{10}B(n,\alpha)^7Li$ (boron dose) are implemented at the VITA accelerator neutron source created at Budker Institute of Nuclear Physics (Siberian Branch, Russian Academy of Sciences) for boron neutron capture therapy [3]. The proposed system uses two types of sensors: the first is based on the SC-331 scintillator, enriched with boron, the second is based on the SC-301 scintillator, which has a similar chemical composition but without boron. These scintillators were developed and manufactured at the Logunov Institute for High Energy Physics in Protvino [4]. The light signal from the sensor is transmitted via a fiber optic cable to a micropixel avalanche photodiode, and the registration electronics increment the event counter when the signal exceeds a threshold of several optical photons. The magnitude of the neutron flux is determined by the difference in counts between the two sensors. This approach allows us to exclude the influence of extraneous factors and measure neutron fluxes at the level of the electronics' own noise up to several hertz.

Another method of radiation therapy that is quite widespread in the world is proton therapy. Despite extensive experience in its clinical use, the search for methods to increase its effectiveness through radiation-related effects continues. To this end, issues of

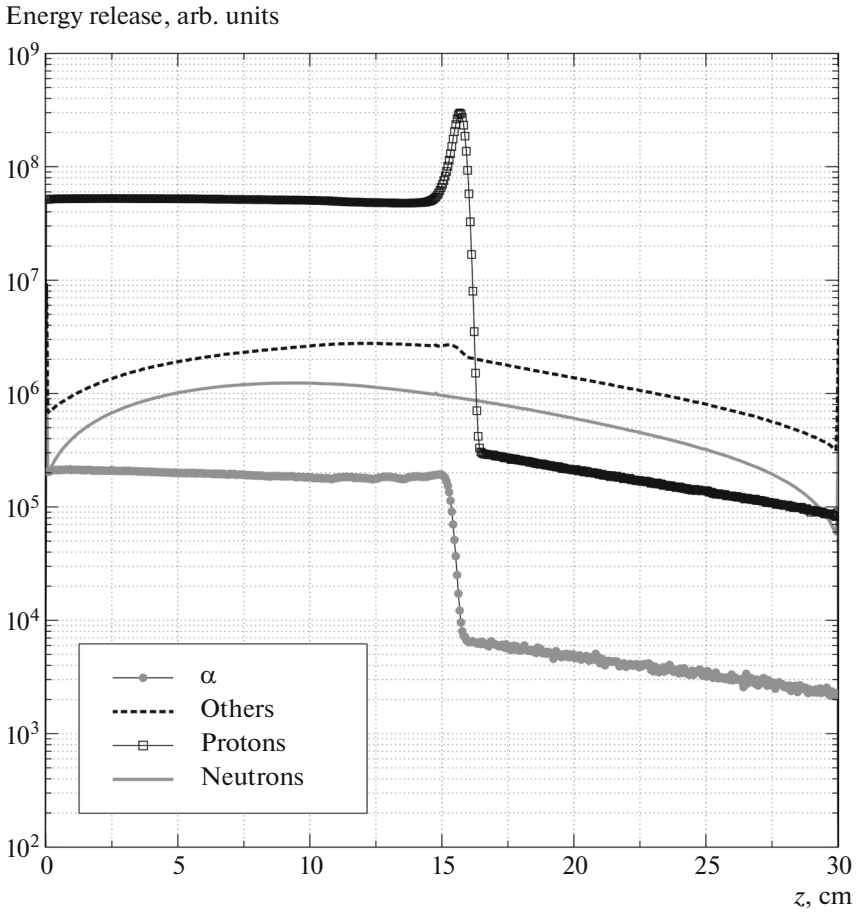

Fig. 1. Calculated value of the relative contribution to the energy release (dose) in a water phantom from protons, alpha particles, and other reaction products.

enhancing the biological effectiveness of therapy through the additional use of special drugs are being actively studied. Thus, in [5], the authors observed the effect of enhancing therapy when using boron-containing drugs, which they associated with the possible significant contribution of reaction products $^{11}B + p \rightarrow 3\alpha + 8.7$ MeV. An alternative hypothesis is that the effect is enhanced by the reaction $^{10}B(n, \alpha)^7Li$ since it is generally accepted that neutrons initially make a small contribution to the absorbed dose for the patient [6]. Since our detectors use a boron-enriched scintillator, we can directly attempt to detect these effects.

2. SIMULATION OF PROTON IRRADIATION

To estimate the magnitude of the expected effect, we performed Monte Carlo calculations of dose distributions in a $30 \times 30 \times 30$ cm^3 water phantom when irradiated with a directed proton beam using theGeant4 v. 11.2.2 modeling package (https://geant4.web.cern.ch/). In the calculations, 10^8 primary particles with an energy of 150 MeV were generated, and the beam shape was described by a Gaussian distribution with $\sigma = 3$ mm. Figure 1 shows the integral distribution of energy release by phantom depth from protons and alpha particles as well as the contribution from other nuclear reaction products. In the region of the Bragg peak, it can be seen that the contribution of alpha particles to the radiation dose is almost three orders of magnitude less than the contribution of protons.

Figure 2 additionally shows the calculated spectra of energy release in the region of the Bragg peak (at a depth of 15 cm), in scintillators with and without boron from protons (N1p, N2p), alpha particles (N1α, N2α), and other particles (N1o, N2o) for sensors located along the beam axis. It follows from the presented data that there is no obvious difference in the spectra between the two types of scintillators, despite the fact that the mass fraction of natural boron is 4.5% in the SC-331 scintillator, which is many orders of magnitude higher than the clinical dose of boron-containing drugs accumulated in tissues. A small peak with an energy of approximately 1.472 MeV present in the spectra of the boron scintillator should be attributed to the $n + {}^{10}B \rightarrow \alpha + {}^7Li$

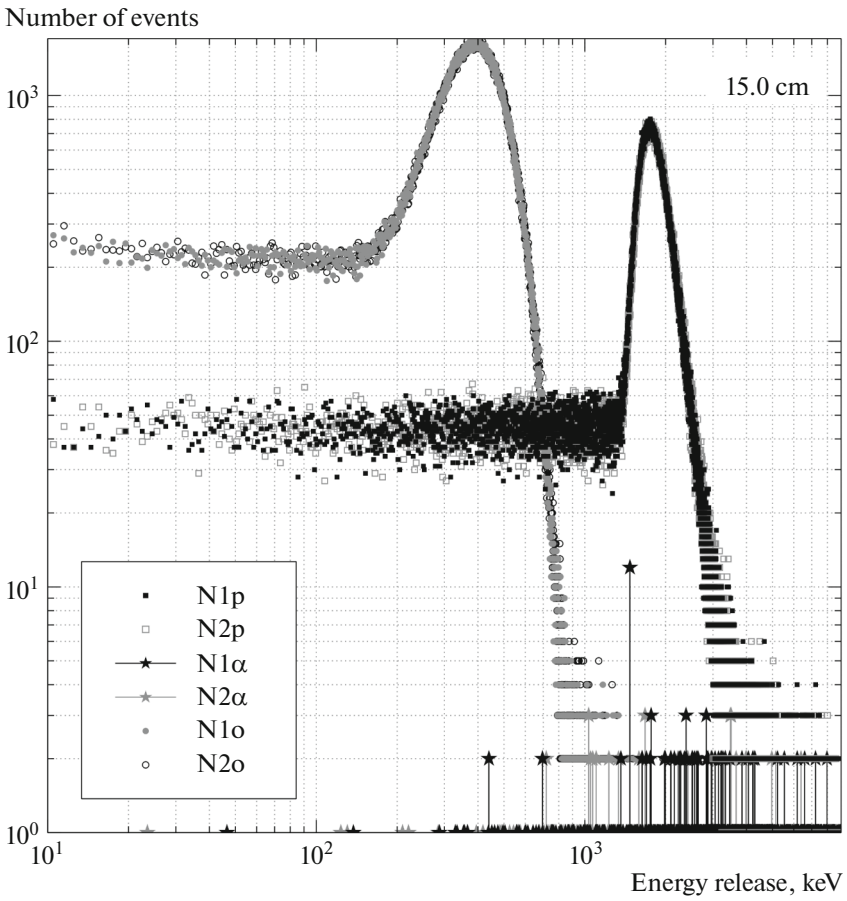

Fig. 2. Energy release spectra in scintillators for particles of different types at a depth of 15 cm for the sensors. N1 and N2 correspond to a scintillator with and without boron, p are protons, α are alpha particles, o are others.

reaction since it produces an alpha particle with a kinetic energy of 1.472 MeV and a Li ion with a kinetic energy of 0.84 MeV. Even though we used 10^8 particles in the calculations, which is comparable to the actual proton flow during therapy, no additional noticeable sources of alpha particle formation are observed [7, 8].

It should be noted that the Geant4 modeling package includes various models of physical processes that can be combined depending on the user's tasks; these models use both analytical expressions and tabulated experimental data to calculate interaction cross-sections. One of the standard sets of physical models, QGSP_BIC_HP, is recommended for calculations in dosimetric and medical problems [9]. Moreover, the cross sections of the reactions of inelastic interaction of protons in different models differ and, in general, have discrepancies with the values observed in experiments [10]. The results of this work were obtained using a standard set of physical models, QGSP_BIC_AllHP, which is an extended version of QGSP_BIC_HP, and additionally uses data on the inelastic interaction of protons and low-energy light ions from the TENDL nuclear reaction library. As an example, Fig. 3 shows the total cross section of the inelastic interaction of protons with boron from Geant4 using various physical models and, separately, the experimentally obtained cross section of the $^{11}B + p \rightarrow 3\alpha + 8.7$ MeV reaction [11]. Although the reaction cross-section at energies below 1 MeV for the standard sets of Geant4 physical models shows a significantly smaller value than that observed in the experiment, the QGSP_BIC_AllHP set has a closer cross-section value than the others, which suggests that the calculations performed using it give plausible results. Thus, the possible contribution to the radiation dose from the reaction $^{11}B + p \rightarrow 3\alpha + 8.7$ MeV can be considered insignificant, and, to obtain a noticeable effect, a significantly higher concentration of boron-containing drugs in tissues is required than is actually used in practice. A similar conclusion was obtained in [12, 13].

3. PROTON BEAM MEASUREMENTS

To experimentally test the possibility of using the developed sensors to measure the fluxes of neutrons generated during the irradiation of objects at proton accelerators, experiments were conducted using the

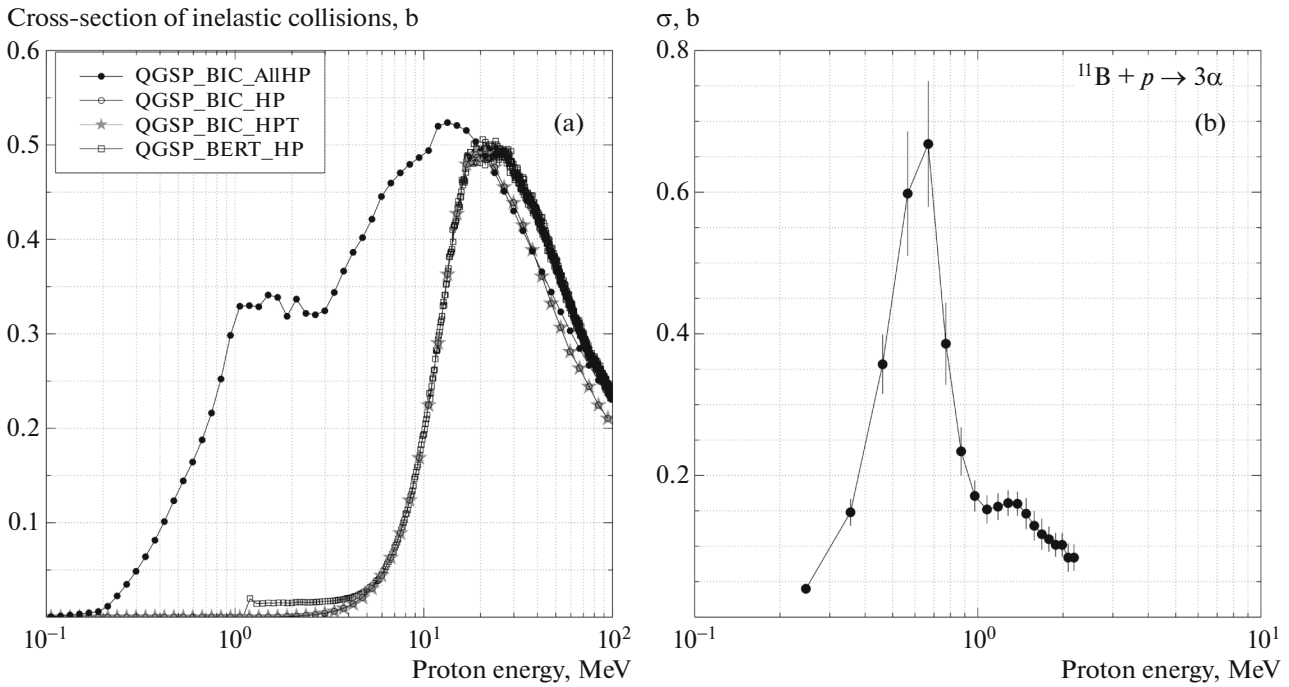

Fig. 3. (a) Cross section of inelastic interaction of protons with boron atoms for four different standard sets of physical models of the Geant4 package and (b) the experimentally obtained value of the cross section for the reaction $^{11}B + p \rightarrow 3\alpha + 8.7$ MeV.

Prometheus proton therapy complex at the shared use center of the Physicotechnical Center, Lebedev Physical Institute, Russian Academy of Sciences (Protvino). This complex implements the technique of irradiation with a narrow "pencil" beam. The size of the input beam in the orthogonal plane is described by a Gaussian distribution with $\sigma \sim 3$ mm at proton energy of 150 MeV. Figure 4 shows a photograph of the water phantom and the location of the sensors installed in the experiment. Sensor C was mounted stationary on the rear wall of the phantom, while sensors A and B moved inside the water volume. Sensor A was an optical fiber without a scintillator installed on it. The use of such an additional sensor makes it possible to estimate the contribution of Cherenkov radiation generated by the electrons formed in the fiber material. The beam-release mode used during operation was 6×10^8 protons in a pulse lasting 300 ms. High input loads and limited response time of the detector operating in counting mode did not allow measurements to be taken directly inside the beam, so all measurements were carried out at some distance from its axis.

The large proton flux gradients observed in the experiment and the relatively large distance between the sensors (4 mm) did not allow for an unambiguous interpretation of the difference signal between the sensors near the beam. At the same time, at large distances from the beam and beyond the Bragg peak, a signal from scattered neutrons is observed at a level of 10–50 events, which coincides with the expected value obtained from the simulation. An example of two-dimensional scanning along the beam and, separately, the result of scanning at a distance of 25 mm along its axis are shown in Fig. 5. This figure shows the count in the registration channel of the sensor without boron, Bg, the difference signal between the two sensors (neutrons), Bn, the difference signal (neutrons) in the fixed sensor on the rear wall of the phantom, Cn, and the signal in the sensor without scintillators, A. In the readings of the fixed sensor C, a burst of neutron generation is visible when sensors A and B pass through the Bragg peak. In addition, a surge in readings in sensor A, which records Cherenkov radiation generated in the light guide, indicates a noticeable generation of high-energy gamma radiation in the same area. The most likely candidates for the origin of this surge are reactions $^{11}B(p, n)^{11}C$ (cross-section approximately 500 mb), $^{12}C(p, p + n)^{11}C$, $^{12}C(p, \gamma)^{13}N$, and $^{19}F(p, \alpha\gamma)^{16}O$ since the design of the sensor housing contains these substances in noticeable quantities.

4. CONCLUSIONS

Based on the data obtained in the simulations using the Geant4 package using the QGSP_BIC_AllHP set of physical models, the mechanism of enhancing biological efficiency observed in studies [6] due to the reaction $^{11}B + p \rightarrow 3\alpha + 8.7$ MeV is questionable due to the significantly smaller contribution to the radiation dose from alpha particles compared to protons

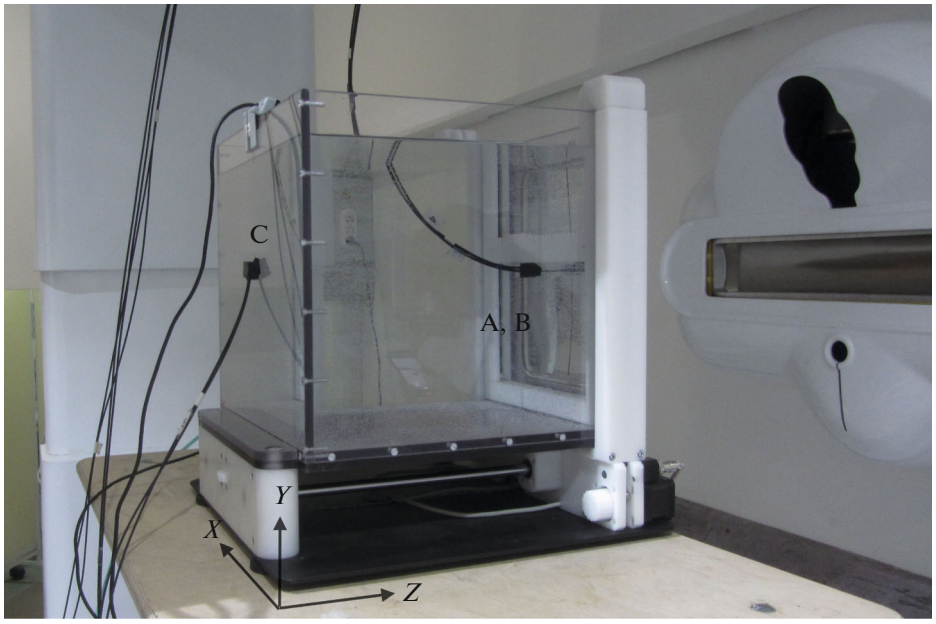

Fig. 4. Photograph of the water test object on the Prometheus proton therapy complex. The locations of sensors A, B, and C are shown.

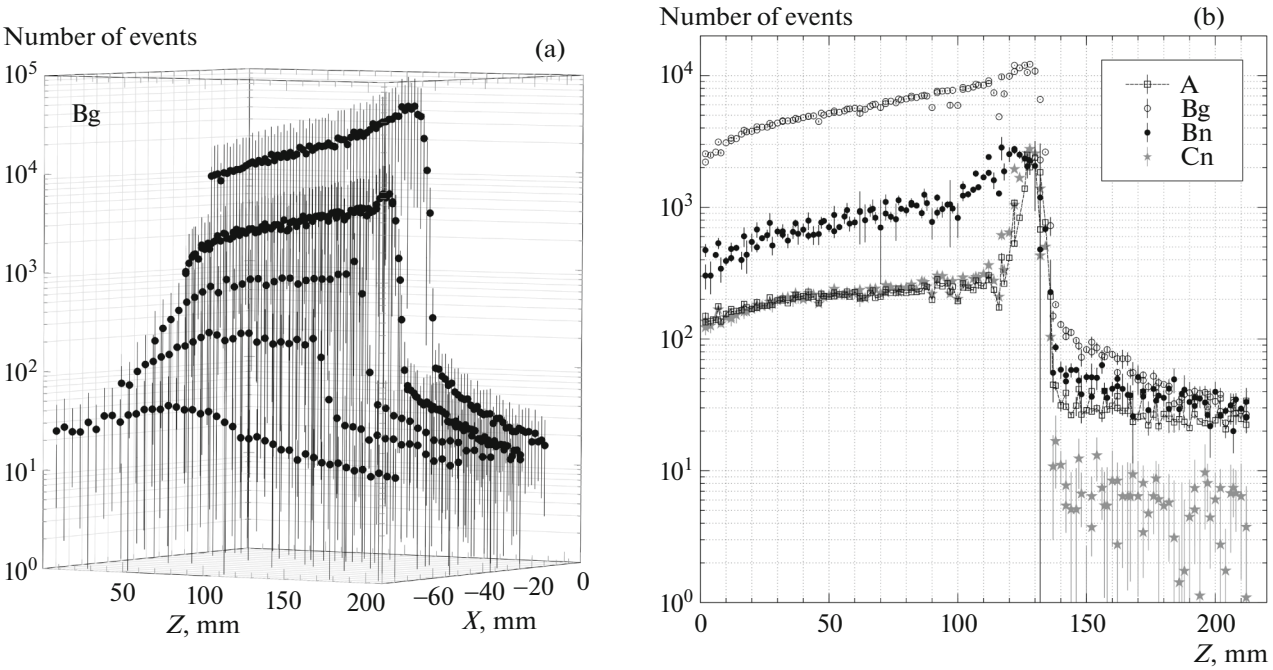

Fig. 5. (a) Dependence of the signal in the Bg channel (sensor B, scintillator without boron) during two-dimensional scanning along the proton beam and (b) signals in the registration channels of sensors A (without scintillators), Bg (sensor B, scintillator without boron), Bn (sensor B, difference signal between channels with different types of scintillators), and Cn (sensor C, difference signal between channels with different types of scintillators) when scanning at a distance of 25 mm from the beam axis.

and other reaction fragments. The experimentally determined values of thermal neutron fluxes are in good agreement with the calculation results and also cannot make a noticeable contribution to the radiation dose due to the reaction $^{10}B(n, \alpha)^7Li$. Large gradients of dose fields in proton beams do not allow the use of the developed sensors to measure the cross-sections of individual reactions involving them. However, the

developed flow-monitoring system can be used to measure the parameters of proton beams in a water phantom. The effects observed in the experiment indicate a noticeable generation of secondary particles when the sensors are located at the Bragg peak, which leads to the conclusion that it is necessary to carefully select the chemical composition of the materials falling within the irradiation zone. Thus, further study of this issue and the search for alternative mechanisms explaining the observed effect of enhancing the biological effectiveness of therapy are necessary.

FUNDING

The study was supported by the Russian Science Foundation (grant no. 19-72-30005, https://rscf.ru/project/19-72-30005/). Proton irradiation was carried out at the Collective Use Center based at the Prometheus proton therapy complex of the Physicotechnical Center (Lebedev Physical Institute, Russian Academy of Sciences) in Protvino.

CONFLICT OF INTEREST

The authors of this work declare that they have no conflicts of interest.

REFERENCES

1. Ishikawa, M., Yamamoto, T., Matsumura, A., et al., *Radiat. Oncol.,* 2016, vol. 11, p. 105. https://doi.org/10.1186/s13014-016-0680-0
2. Ishikawa, M., Ono, K., Sakurai, Y., et al., *Appl. Radiat. Isot.,* 2004, vol. 61, no. 5, p. 775. https://doi.org/10.1016/j.apradiso.2004.05.053
3. Bykov, T.A., Kasatov, D.A., Koshkarev, A.M., et al., *J. Instrum.,* 2021, vol. 16, p. 01024. https://doi.org/10.1088/1748-0221/16/01/P01024
4. Britvich, G.I., Vasil'chenko, V.G., Gilitsky, Yu.V., et al., *Instrum. Exp. Tech.,* 2004, vol. 47, p. 571. https://doi.org/10.1023/B:INET.0000043862.12092.b0
5. Cirrone, G.A.P., Manti, L., Margarone, D., et al., *Sci. Rep.,* 2018, vol. 8, p. 1141. https://doi.org/10.1038/s41598-018-19258-5
6. Halg, R.A. and Schneider, U., *Br. J. Radiol.,* 2020, vol. 93, no. 1107, p. 20190412. https://doi.org/10.1259/bjr.20190412
7. Becker, H.W., Rolfs, C., and Trautvetter, H.P., *Z. Phys. A: At. Nucl.,* 1987, vol. 327, p. 341. https://doi.org/10.1007/BF01284459
8. Dmitriev, V.F., *Phys. At. Nucl.,* 2009, vol. 72, p. 1165. https://doi.org/10.1134/S1063778809070084
9. Arce, P., Bolst, D., Bordage, M.-C., et al., *Med. Phys.,* 2021, vol. 48, no. 1, p. 19. https://doi.org/10.1002/mp.14226
10. Arce, P., Archer, J.W., Arsini, L., et al., *Med. Phys.,* 2025, vol. 52, p. 2707. https://doi.org/10.1002/mp.17678
11. Taskaev, S., Bessmeltsev, V., Bikchurina, M., et al., *Nucl. Instrum. Methods Phys. Res., Sect. B,* 2024, vol. 555, p. 165490. https://doi.org/10.1016/j.nimb.2024.165490
12. Mazzone, A., Finocchiaro, P., Meo, S.L., and Colonna, N., *Eur. Phys. J. Plus.,* 2019, vol. 134, p. 361. https://doi.org/10.1140/epjp/i2019-12725-8
13. Geser, F.A. and Valente, M., *Appl. Radiat. Isot.,* 2019, vol. 151, p. 96. https://doi.org/10.1016/j.apradiso.2019.04.034